

Performance evaluation of glucose oxidation reaction using biocatalysts adopting different quinone derivatives and their utilization in enzymatic biofuel cells

Kyuhwan Hyun[‡], Suhyeon Kang[‡], and Yongchai Kwon[†]

Graduate School of Energy and Environment, Seoul National University of Science and Technology,
232 Gongneung-ro, Nowon-gu, Seoul 01811, Korea
(Received 22 October 2018 • accepted 20 December 2018)

Abstract—Glucose oxidase (GOx) and four different quinone derivatives (p-benzoquinone (BQ), naphthoquinone (NQ), anthraquinone (AQ) and 1,5-Dihydroxyanthraquinone (15DHAQ)) based biocomposites were embedded in polyethyleneimine (PEI) and then immobilized on carbon nanotube (CNT) substrate (CNT/PEI/Quinone/GOx). These catalysts were then used as the anodic biocatalysts for the enzymatic biofuel cell (EBC). According to the performance investigations of catalysts, the catalytic activity for glucose oxidation reaction (GOR) representing the electron transfer rate between GOx and glucose fuel is mostly enhanced in CNT/PEI/NQ/GOx. It is because two benzene rings of NQ play a role in attracting and releasing electrons effectively, increasing the catalytic activity for GOR, while other quinones have problems about attracting electrons (AQ and 15DHAQ) and wrong position of the reactive site for electron transfer (BQ). Excellent electron transfer rate constant (1.1 s^{-1}) and Michaelis-Menten constant (0.99 mM) are outstanding evidence for that. Furthermore, when the catalyst is utilized for EBC, high power density ($57.4 \mu\text{Wcm}^{-2}$) and high open circuit voltage (0.64 V) are accomplished.

Keywords: Glucose Oxidase, Quinone Derivatives, Enzymatic Biofuel Cell, Polyethylenimine, Naphthoquinone

INTRODUCTION

Glucose oxidase (GOx) is an enzyme containing flavin adenine dinucleotide (FAD) as co-factor, while this oxidizes glucose as gluconolactone and reduces oxygen (O_2) as hydrogen peroxide (H_2O_2) simultaneously. Since the glucose oxidation reaction (GOR) that represents a reaction between FAD and glucose can induce excellent electromotive force (EMF) and the glucose has superior selectivity to GOx for GOR, considerable efforts have been made to adopt this reaction as a main anodic reaction of enzymatic biofuel cells (EBCs) [1-3]. Due to such a high EMF, the power density of EBCs increases, while by the superior selectivity of glucose, electricity can be stably produced even in the less-pure and impurity-contained states of glucose fuel [4,5].

In terms of GOR, O_2 molecules can play a crucial role in attracting electrons and protons. However, it is difficult for them to be used as a mediator for transferring electrons and protons because their electron affinity is high (0.448 eV), meaning that they do not easily release electrons and protons to electrode [6-8]. In addition, the oxidation reactions linked to the O_2 molecules occur at too positive potentials. For instance, onset potential for the oxidation reaction of H_2O_2 ($\text{H}_2\text{O}_2 \rightarrow \text{O}_2 + 2\text{H}^+ + 2\text{e}^-$) is 0.70 V vs. SHE and that for the reduction reaction of O_2 ($\text{O}_2 + 4\text{H}^+ + 4\text{e}^- \rightarrow 2\text{H}_2\text{O}$) is 1.23 V vs. SHE [13]. Thus, thermodynamically, when O_2 is used, the maximum onset potential of EBC is just 0.53 V, and this is approximately half

that of PEMFC (1.23 V). This fact indicates that oxidation reaction using O_2 mediator is not effective to produce a high cell potential, followed by an excellent power density of EBC [9-12].

To address this issue of oxidation reaction using O_2 mediator, a new artificial mediator that has a lower electron affinity than O_2 molecules and can induce the oxidation reactions in a low potential range should be developed. With the development of new artificial mediator, releasing the electrons and protons can be more facilitated and then appropriate electron shuttling by the mediator is possible.

Based on that, benzene-based chemicals are a good candidate because their electron affinity is very low (-1.15 eV), and when hydrogen atoms tied to the outer shell of the chemicals are substituted with other atoms, its electron affinity can be easily controlled [13]. In this prospect, quinone derivatives substituting the hydrogen of benzene into the oxygen can be considered for the purpose as artificial mediator. Since quinone has a lower the electron affinity than O_2 molecules, in terms of the capability of attracting electrons that are contained in FADH_2 (reduced form of FAD), the quinone derivatives have a lower attraction force than O_2 molecules. However, for the same reason, the electrons contained in the quinone derivatives are easily released to the electrode [13-15].

In addition, according to Gorner et al., who compared the electron attracting force of quinone derivatives with that of O_2 molecules, when the reduction reaction of biocatalysts containing the quinone derivatives occurs ($\text{Quinone}^- + \text{O}_2 \rightarrow \text{Quinone} + \text{O}_2^-$), their reaction equilibrium constant, K , is clearly different. For instance, in three quinone derivatives of p-benzoquinone (BQ), naphthoquinone (NQ), anthraquinone (AQ), K of NQ is higher than that of other quinones (K value of BQ, AQ are $(0.5-1) \times 10^{-9} \text{ M}^{-1} \text{ s}^{-1}$, and that of NQ is $(1-4) \times 10^{-7} \text{ M}^{-1} \text{ s}^{-1}$), which means that the electron

[†]To whom correspondence should be addressed.

E-mail: kwony@seoultech.ac.kr

[‡]These authors are equally contributed to this work.

Copyright by The Korean Institute of Chemical Engineers.

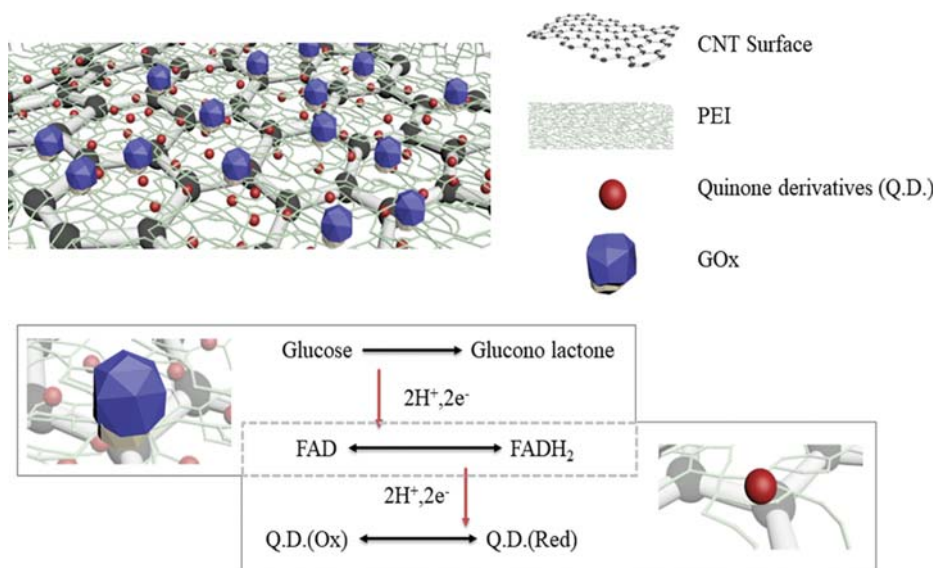


Fig. 1. Schematic illustration showing (i) CNT/PEI/Quinone/GOx biocatalyst, and (ii) the reaction mechanism of oxidation reactions (anodic reactions), including glucose oxidation reaction.

attraction force of NQ is probably 20-25 times weaker than that of other quinones [16,17].

To investigate the potential of NQ as the mediator of oxidation reactions for EBC, a new GOx based biocatalysts was studied. For the preparation of biocatalyst, GOx and four different quinone derivatives (BQ, NQ, AQ and 1,5-Dihydroxyanthraquinone (15DHAQ)) based biocomposites are embedded in polyethyleneimine (PEI), and they are then immobilized onto carbon nanotube (CNT) substrate to complete CNT/PEI/Quinone/GOx biocatalysts. Here, four different quinone derivatives are proposed as a new artificial mediator because quinone derivatives are relatively cheap and electron shuttling capability is excellent, while their redox reaction potentials are within a sufficient range for the oxidation reactions (or anodic reactions), including GOR [18-20].

For measuring the catalytic activity of the biocatalysts including cell potential and reaction rate, and comparing the performance of biocatalysts one another, different characterizations are carried out. Cyclic voltammogram (CV) is considered to inspect the catalytic activity and performance of biocatalysts, such as the electron transfer rate constant, the Michaelis-Menten constant and biosensor sensitivity, while cell potential and power density of EBCs using the biocatalysts are obtained by measuring their polarization curves.

EXPERIMENTAL

1. Materials

Multiwall carbon nanotubes (MWCNT, MR99, Average diameter 20 nm, purity is higher than 99%) were obtained from Carbon NanoTech (Gyeongbuk, Korea). Glucose oxidase (GOx, from *Aspergillus niger* type X-S, 150,000 U·g⁻¹ solid) and Polyethyleneimine (PEI, 50% (w/v) solution in water, MW 750,000) glucose (ACS reagent) p-benzoquinone, naphthoquinone, anthraquinone, 1,5-Dihydroxyanthraquinone, Nafion solution (70160) were purchased from Sigma Aldrich (Milwaukee, WI, USA).

2. Synthesis of CNT/PEI/Quinone/GOx Biocatalysts

Fig. 1 schematically illustrates the chemical structure and glucose fueled reaction mechanism of synthesized CNT/PEI/Quinone/GOx biocatalysts, and their synthesis proceeded with the following procedure. 1 mg of quinone was initially mixed with 1 mL of 5 mg·mL⁻¹ PEI solution, and the solution including PEI and quinone was stirred for 1 h to immobilize as many as possible the quinone molecules onto the PEI surface. Such synthesized PEI/Quinone composite was then mixed with 1 mL of 2 mg·mL⁻¹ CNT solution with the sonication of 10 min and was then stirred for 1 h. With the process, the physical entrapment between PEI/Quinone composite and CNT occurred. After stirring, the remaining PEI/Quinone composite that was not immobilized onto the CNT was removed. In turn, the CNT/PEI/Quinone powder was mixed with 5 mg·mL⁻¹ GOx solution with the sonication of 10 min and was then stirred for 30 h for another physical entrapment between CNT/PEI/Quinone and GOx. With the procedure, four different CNT/PEI/Quinone/GOx biocatalysts (CNT/PEI/BQ/GOx, CNT/PEI/NQ/GOx, CNT/PEI/AQ/GOx, and CNT/PEI/15DHAQ/GOx) were fabricated.

3. Electrochemical Characterization Including EBC Full Cell Test

The electrochemical measurements were performed in a potentiostat (BioLogic SP-240, USA). For the half-cell measurements, Pt wire and Ag/AgCl (soaked in 3.0 M NaCl) were regarded as the counter and reference electrodes, and the biocatalyst ink coated glassy carbon electrode (GCE) was used as working electrode with an active electrode area of 0.2 cm². To prepare the working electrode, 10 μL of catalytic ink was loaded onto the GCE and then the catalytic ink loaded GCE was dried under room temperature. After dry, 5 wt% Nafion solution was further loaded onto the catalytic ink-loaded GCE [1,21,22]. Phosphate buffer solution (PBS) was considered as an electrolyte for facilitating the FAD/FADH₂ redox reaction within GOx, and high purity N₂ and air gases were

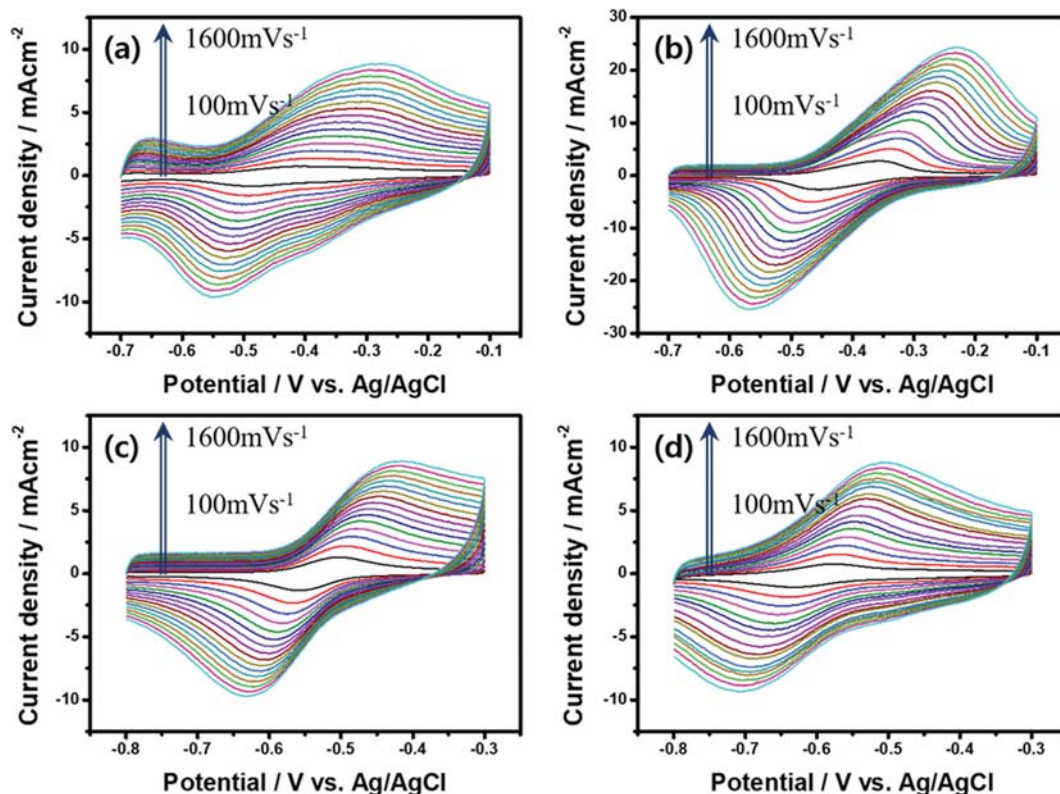


Fig. 2. Cyclic voltammograms (CV) of (a) CNT/PEI/BQ/GOx (b) CNT/PEI/NQ/GOx (c) CNT/PEI/AQ/GOx (d) CNT/PEI/15DHAQ/GOx. For CV tests, 10 mM phosphate buffer solution (pH 7.4) was used as electrolyte under N_2 state; the potential scan rate was from 100 to 1,600 mVs^{-1} .

fed to the electrolyte to make N_2 -state and air-state conditions.

To measure the polarization curves of EBC single cells, an in-house EBC kit was used. Its active area was 1 cm^2 and $20\ \mu\text{L}$ of the corresponding biocatalyst was loaded onto GCE and the GCE was used as the anode electrode, while the cathodic catalyst containing 3.33 mg of platinum on carbon (Pt/C, 20 wt%) was sprayed onto Nafion 117 membrane. As for the anode fuel, 0.1 M glucose solution (1x, PBS pH 7.4) was rotated from an external reservoir to the EBC kit at a flow rate of 0.1 mL min^{-1} , while O_2 gas was supplied as the fuel for cathodic reaction at a flow rate of 50 cc min^{-1} .

RESULTS AND DISCUSSION

1. Electrochemical Evaluations of CNT/PEI/Quinone/GOx Biocatalysts

A catalyst using NQ as entrapped artificial mediator (CNT/PEI/NQ/GOx) was fabricated and for the purpose of comparison, the catalysts using other entrapped artificial mediators like AQ, BQ, and 15DHAQ (CNT/PEI/BQ/GOx, CNT/PEI/AQ/GOx and CNT/PEI/15DHAQ/GOx) were also synthesized.

To make a strong link between GOx and quinones, PEI, which is an entrapping polymer and CNT substrate were also adopted [23,24]. The PEI is a polymer containing multiple amine groups and has a dendrite shape [25,26]. With the amine groups, PEI can have a high isoelectric point (10.4), and its dendrite shape plays a role in facilitating the bonding with other materials. Thus, with use

of the PEI, the quinone substituents, as well as GOx molecules, can be appropriately captured, alleviating leaching-out of the quinone and GOx molecules [1,22].

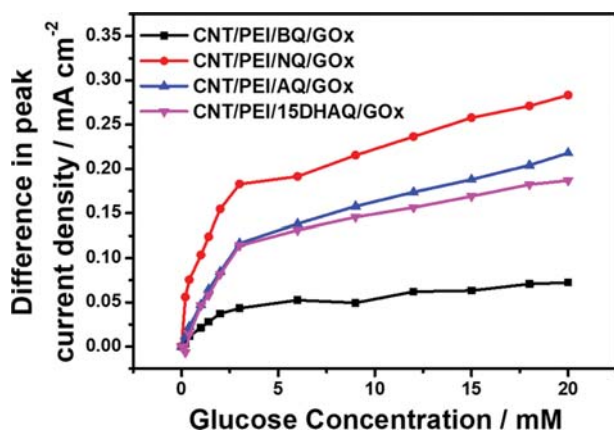
To investigate the reduction potential and current density of CNT/PEI/Quinone/GOx, CV curves were measured and the related results are shown in Fig. 2. The redox current density peak observed in $-0.61\sim-0.40\text{ V vs. Ag/AgCl}$ of Fig. 2 represents the reaction between FAD within GOx and quinone. Namely, by the utilization of the different quinone derivatives, the current density and peak potential of CNT/PEI/Quinone/GOx were varied and the difference was measured [27].

There are two notable findings to be reported from Fig. 2. First, when the peak current of the biocatalysts was measured in the same scan rate of 10 mVs^{-1} , the current value of NQ, BQ, AQ and 15DHAQ was recorded as 6.1, 1.7, 3.8 and $0.4\times 10^{-5}\text{ Acm}^{-2}$, meaning that NQ showed 1.6-15.3-times higher peak current value than other biocatalysts. This implies that the redox reactivity of NQ/GOx composite is better than that of other quinone/GOx composites. Second, the CV curve of CNT/PEI/BQ/GOx biocatalyst showed two distinctive reduction reaction peaks. It explains that the electron transfer between FAD and BQ did not properly proceed, and as a result, the reduction reaction peaks for (i) between FAD and BQ and (ii) BQ itself were separately observed [27].

Based on Fig. 2, the electron transfer rate constant (k_s) of the CNT/PEI/Quinone/GOx biocatalysts was also calculated using Laviron's equation [1]. The data is summarized in Table 1.

Table 1. k_s and k_m values of CNT/PEI/BQ/GOx, CNT/PEI/NQ/GOx, CNT/PEI/AQ/GOx, CNT/PEI/15DHAQ/GOx

	CNT/PEI/BQ/GOx	CNT/PEI/NQ/GOx	CNT/PEI/AQ/GOx	CNT/PEI/15DHAQ/GOx
k_s (s^{-1})	1.2449	1.0455	1.8912	1.9718
k_m (mM)	2.08	0.99	3.56	5.38

**Fig. 3.** Michaelis-Menten curves calculated from four different biocatalysts (CNT/PEI/BQ/GOx, CNT/PEI/NQ/GOx, CNT/PEI/AQ/GOx, and CNT/PEI/15DHAQ/GOx). For the tests, 0-20 mM of glucose was dissolved in 0.01 M PBS (pH 7.4) and potential scan rate was 100 mVs⁻¹.

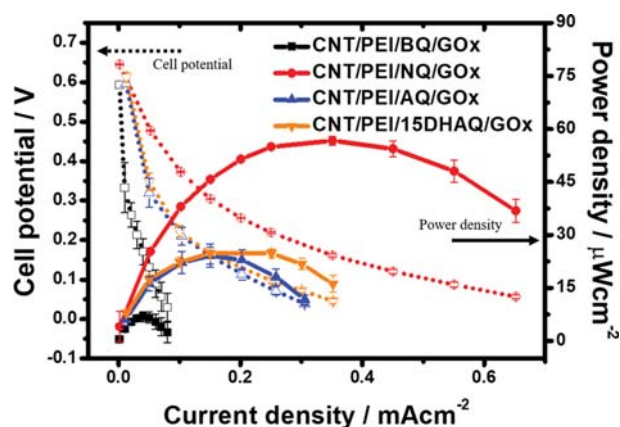
When k_s of the four different biocatalysts were compared, that of CNT/PEI/NQ/GOx was highest, while that of CNT/PEI/AQ/GOx was lowest. This result demonstrates that BQ molecules are distributed to the outside of biocatalyst and electron transfer is not activated, while NQ molecules are evenly distributed within the biocatalyst and electron transfer is relatively promoted [27].

As another important parameter to determine the availability of biocatalysts, investigating the reactivity of biocatalysts for the reaction with glucose in actual operating condition is important, and this is measured using CV curves. For the tests, the scan rate of 50 mVs⁻¹ was used, while PBS (pH 7.4) was used as the electrolyte. According to a detailed experimental procedure, glucose was injected gradually from 0 to 20 mM to the electrolyte, observing the change in reduction reaction peak of the corresponding CV curves (Fig. 3) [1]. All four biocatalysts showed superior glucose sensitivity until the injection of 4 mM glucose, and then the glucose sensitivity was less accurate in the glucose concentration more than 4 mM.

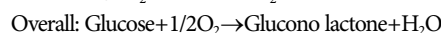
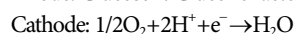
For further investigation, the catalytic activity of biocatalysts using Michaelis-Menten and Lineweaver-Burk equations was evaluated, and the data are summarized in Table 1. In the measurements, K_m of CNT/PEI/NQ/GOx was best (0.99 mM), indicating that redox reaction among PEI, NQ and GOx was mostly promoted.

2. The Performance of EBCs using CNT/PEI/Quinone/GOx Biocatalysts

We investigated the performance of EBCs using CNT/PEI/Quinone/GOx and Pt/C as anodic and cathodic catalysts by measuring their polarization curves. As for fuel, glucose and O₂ gas were used and Nafion 117 was considered as separator [9,28-30]. The polarization curves were measured three times to ensure the reproducibility of corresponding tests.

**Fig. 4.** Polarization curves of the EBCs including the CNT/PEI/BQ/GOx, CNT/PEI/NQ/GOx, CNT/PEI/AQ/GOx, and CNT/PEI/15DHAQ/GOx as anodic catalysts and Pt/C as a cathodic catalyst. In the tests, 40 mM glucose was fed as a fuel from an outside reservoir to the anode of the EBC kit at a flow rate of 0.1 mLmin⁻¹ and 50 cc min⁻¹ of O₂ gas was supplied to the cathode.

The overall reaction mechanism is represented as follows:



The detailed mechanism of anode reaction, explained in Fig. 2, indicates that the electrons and protons produced from glucose are transferred to quinone via FAD within GOx, and such oxidized quinone transfers the electrons into the electrode and the protons into membrane. In turn, the electrons and protons are headed into the cathode, completing the redox reaction for EBC operation.

According to the polarization curves (Fig. 4), the maximum power density (MPD) and cell potential of EBC using CNT/PEI/NQ/GOx biocatalyst were highest as 56.6±1.21 μWcm⁻² and 0.64 V, while that of EBC using CNT/PEI/BQ/GOx biocatalyst was lowest as 6.9±1.37 μWcm⁻² and 0.59 V. Furthermore, in the EBCs using CNT/PEI/AQ/GOx and CNT/PEI/15DHAQ/GOx biocatalysts their MPD was similar as ~26 μWcm⁻², while their cell potential was 0.60 V (CNT/PEI/AQ/GOx) and 0.61 V (CNT/PEI/15DHAQ/GOx). Such MPD and onset potential trend supports that NQ plays a crucial role in improving a desirable GOR by promoting electron transfer. As shown even in the half-cell experiment, it is due to the two benzene ring structure of NQ that attracts and releases electrons effectively, increasing the catalytic activity for GOR and reducing its overpotential.

CONCLUSIONS

We synthesized biocatalysts containing four different quinone

derivatives (BQ, NQ, AQ, and 15DHAQ) for promoting oxidation reaction (anodic reaction), which is a rate-determining reaction for EBC that represents the electron transfer rate between FAD within GOx and glucose fuel. For immobilizing the quinone molecules stably and improving the electron conductivity of biocatalysts, the quinone substituents were embedded in PEI and then immobilized onto CNT substrate to finalize CNT/PEI/Quinone/GOx biocatalysts, and the four different biocatalysts (CNT/PEI/BQ/GOx, CNT/PEI/NQ/GOx, CNT/PEI/AQ/GOx, and CNT/PEI/15DHAQ/GOx) were prepared and compared for their catalytic activity and stability as well as EBC performance. According to the electrochemical characterizations and EBC performance evaluations, the electron transfer rate between FAD within GOx and glucose fuel, which is the main anodic reaction, was mostly improved in CNT/PEI/NQ/GOx. It was because two benzene rings of NQ played a crucial role in attracting and releasing electrons effectively, whereas other quinones had problems about attracting electrons (AQ and 15DHAQ) and wrong position of the reactive site for electron transfer (BQ). In a comparison of the kinetics of the four biocatalysts, CNT/PEI/NQ/GOx showed excellent electron transfer rate constant (1.1 s^{-1}) and Michaelis-Menten constant (0.99 mM). Eventually, when the CNT/PEI/NQ/GOx was utilized as the anodic biocatalyst for EBC, the EBC showed a high power density ($57.4 \mu\text{Wcm}^{-2}$) and high cell potential (0.64 V).

ACKNOWLEDGEMENTS

This work was supported by the National Research Foundation of Korea (NRF) and the Ministry of the Ministry of Education (MOE) (No. 2018R1D1A1A09036711), and by the Korea National Research Foundation (KNRF) and the Ministry of Science, ICT and Future Planning (MSIP) (No. 2016M1A2A2937143) and by the Korea Institute of Energy Technology Evaluation and Planning (KETEP) and Ministry of Trade, Industry & Energy (MOTIE) of Republic of Korea (No. 20184030202230).

REFERENCES

1. K. H. Hyun, S. W. Han, W. G. Koh and Y. Kwon, *J. Power Sources*, **286**, 197 (2015).
2. S. D. Minteer, B. Y. Liaw and M. J. Cooney, *Curr. Opin. Biotechnol.*, **18**, 228 (2007).
3. C. Abreu, Y. Nedellec, O. Ondel, F. Buret, S. Cosnier, A. Le Goff and M. Holzinger, *J. Power Sources*, **392**, 176 (2018).
4. K. Hyun, S. W. Han, W. G. Koh and Y. Kwon, *Int. J. Hydrogen Energy*, **40**, 2199 (2015).
5. M. Christwardana, J. Ji, Y. Chung and Y. Kwon, *Korean J. Chem. Eng.*, **34**, 2916 (2017).
6. M. Wooten, S. Karra, M. Zhang and W. Gorski, *Anal. Chem.*, **86**, 752 (2013).
7. M. Šulka, M. Pitoňák, P. Neogrady and M. Urban, *Int. J. Quantum Chem.*, **108**, 2159 (2008).
8. N. Driver and P. Jena, *Int. J. Quantum Chem.*, **118**, e25504 (2018).
9. I. Katsounaros, W. B. Schneider, J. C. Meier, U. Benedikt, P. U. Biedermann, A. A. Auer and K. J. Mayrhofer, *Phys. Chem. Chem. Phys.*, **14**, 7384 (2012).
10. C. Bunte, L. Hussein and G. A. Urban, *J. Power Sources*, **247**, 579 (2014).
11. E. Nazaruk, S. Smoliński, M. Swatko-Ossor, G. Ginalska, J. Fiedurek, J. Rogalski and R. Bilewicz, *J. Power Sources*, **183**, 533 (2008).
12. Y. Wang and Y. Hasebe, *J. Electrochem. Soc.*, **159**, 110 (2012).
13. J. B. Conant and L. F. Fieser, *J. Am. Chem. Soc.*, **46**, 1858 (1924).
14. M. Latifatu, J. H. Park, J. M. Ko and J. Park, *J. Ind. Eng. Chem.*, **63**, 12 (2018).
15. E. Yuan, C. Wu, G. Liu, G. Li and L. Wang, *J. Ind. Eng. Chem.*, **66**, 158 (2018).
16. H. Görner, *Photochem. Photobiol. Sci.*, **3**, 933 (2004).
17. M. J. Lee, N. H. Chun, H. C. Kim, M. J. Kim, P. Kim, M. Y. Cho and G. J. Choi, *Korean J. Chem. Eng.*, **35**, 984 (2018).
18. S. Nawar, B. Huskinson and M. Aziz, *Mater. Res. Soc. Symp. Proc.*, **1491** (2013).
19. M. Uchimiya and A. T. Stone, *Chemosphere*, **77**, 451 (2009).
20. R. D. Milton, D. P. Hickey, S. Abdellaoui, K. Lim, F. Wu, B. Tan and S. D. Minteer, *Chem. Sci.*, **6**, 4867 (2015).
21. J. Ji, H. I. Joh, Y. Chung and Y. Kwon, *Nanoscale*, **9**, 15998 (2017).
22. Y. Chung, K. Hyun and Y. Kwon, *Nanoscale*, **8**, 1161 (2016).
23. M. Razzaghi, A. Karimi, H. Aghdasinia and M. T. Joghataei, *Korean J. Chem. Eng.*, **34**, 2870 (2017).
24. Y. O. Im, S. H. Lee, S. U. Yu, J. Lee and K. H. Lee, *Korean J. Chem. Eng.*, **34**, 898 (2017).
25. K. S. Hwang, H. Y. Park, J. H. Kim and J. Y. Lee, *Korean J. Chem. Eng.*, **35**, 798 (2018).
26. A. A. Adewunmi, S. Ismail, A. S. Sultan and Z. Ahmad, *Korean J. Chem. Eng.*, **34**, 1638 (2017).
27. Y. Ahn, Y. Chung and Y. Kwon, *Korean Chem. Eng. Res.*, **55**, 258 (2017).
28. S. Kang, K. S. Yoo, Y. Chung and Y. Kwon, *J. Ind. Eng. Chem.*, **62**, 329 (2018).
29. C. Noh, S. Moon, Y. Chung and Y. Kwon, *J. Mater. Chem. A*, **5**, 21334 (2017).
30. C. Noh, B. W. Kwon, Y. Chung and Y. Kwon, *J. Power Sources*, **406**, 26 (2018).